First Results on Understanding the Shiny Surfaces of Heat-Treated Chert

Julie Bachellerie, Patrick Schmidt

First results on understanding the shiny surfaces of heat-treated chert

Julie Bachellerie [a], Patrick Schmidt [a, b,c]

[a] TRACES - UMR5608, Université de Toulouse Jean-Jaurès, Maison De La Recherche, 5 Allée Antonio Machado, 31058 TOULOUSE, France

[b] Eberhard Karls University of Tübingen, Department of Early Prehistory and Quaternary Ecology, Schloss Hohentübingen, 72070 Tübingen, Germany.

[c] Eberhard Karls University of Tübingen, Department of Geosciences, Applied Mineralogy, Wilhelmstraße 56, 72074 Tübingen, Germany.

Corresponding author:

Julie Bachellerie (Orcid: *0000-0001-5675-0255*)

Mail: julie.bachellerie@etu.univ-tlse2.fr

Tel: +33 648201902

Abstract

In Europe, intentional heat treatment of silica rocks to improve their knapping quality appeared for the first time during the Solutrean (ca 25.5-23 ka cal BP). The recognition of heat-treated artefacts in assemblages is based on macroscopic criteria like shiny luster. Surface luster or gloss, however, may be prone to observer bias and calls for more objectives measures to quantify it. In this study, we use a laser scanning microscope to measure the micro-relief on surfaces knapped after heat treatment at different temperatures. Our results show the evolution of the roughness of fresh fracture surface as a function of heating temperatures. Roughness appears to be a good proxy for macroscopically observable surface gloss caused by heat treatment. Such Ra measurements even bear the potential to become a new tool for the recognition of heat treatment.

Key-words: Early pyrotechnology; surface luster; 3D surface modeling, Fracture surface analysis; Flint

Introduction

Heat treatment is a process that alters the mechanical properties of rocks. It is mostly applied to silica rocks, where it is known to improve knapping quality. In Europe, this technical innovation appeared for the first time during the Solutrean (ca 25.5-23 cal BP) **(Bordes, 1969)**. The process remains poorly understood, especially in terms of its geographic extent and the heating technique(s) used during the Solutrean. Especially the recognition of heat treatment in archaeological assemblages is not always straightforward. At macroscopic scale, gloss contrast is the only reliable criterion for recognizing intentional heat treatment (**Collins and Fenwick, 1974; Inizan et al., 1995; Rondeau, 1995; Tiffagom, 1998)**. The rationale behind gloss contrast is that removal scars present a "greasy luster" when knapped after heat treatment (thus called postheating removal scars**,** see for

example: **Griffiths et al., 1987)**. When postheating scars are associated with matt surfaces that predate heat treatment (preheating removal scars), pieces are described as showing gloss contrast. Gloss contrast pieces are sometimes called “diagnostic”, as they document pre-heat treatment knapping, the transformation of the material’s fracture properties by heat treatment and knapping afterwards. The overall intensity of the gloss depends on the raw material but also on the temperature reached during heat treatment (Inizan et al., 1976). When observed with the unaided eye, gloss cannot be objectively recorded and different observers may report very different results. Thus, in the absence of gloss contrast, it is not always possible to identify heat-treated pieces based on overall gloss intensity.

Gloss has been reported to be correlated with mechanical properties of the rock during heating (**Schmidt et al., 2019**). It might even be understood as being the consequence of the progressive reduction of intergranular pore space and the defect healing occurring in silica rocks during heating (for these mechanisms see: Schmidt et al., 2012, Schmidt et al., 2011). If this were the case, increasing gloss intensity on fresh knapping scars would be expected to be gradual in the temperature zone where chert is transformed during heat treatment (200-350°C, see: **Schmidt et al., 2011**). Finding gradual change in the range between 200°C and 350°C would provide a first argument for a causal relationship between the known chemical and mechanical transformations (**Schmidt et al., 2011, 2012, 2019**) and the macroscopically observable surface gloss. What we know is that macroscopically observable gloss is caused by changes in the surface relief that affect light scattering from the surface (**Schmidt, 2013**). The smoother a surface, the more light it reflects in a certain direction while a rough surface will scatter it in several directions. The evolution of roughness on the surfaces of homogeneous rocks like chert (mostly made of quartz) should be proportional to their glossy appearance. We therefore indirectly measure surface gloss in this study by acquiring 3D surface models on postheating scars with a laser scanning microscope. We do this in the hope that our surface roughness measurements bear the potential to become a new tool for the recognition of heat treatment.

Materials and methods

We choose 4 types of chert that were regularly used by French Solutrean groups: Bergerac chert (2 blocks from 2 different outcrops), black Senonian chert (2 blocks from 2 different outcrops), Grand Pressigny Turonian chert (1 block) and Cher Valley Turonian chert (1 block) (fig.1). These chert types are well known by, at least, French archaeologists and present various textures and different knapping qualities (**Inizan et al., 1976; Masson, 1981**).

We made a reference collection of unheated and experimentally heat-treated flakes from each chert type. First, 3 flakes were removed from each unheated nodule (5 flakes were removed for one of the samples, Bergerac chert from Mouleydier). Then, we heat-treated all six nodules at 200°C, 300°C and 400°C. The ramp rate was chosen to be relatively slow (0.5°C/min) to avoid excessive heat-fracturing, and the maximum temperature was held for 2 hours (for justification, see: **Schmidt et al., 2016**). The nodules were let for >10 hours in the furnace to cool to room temperature. At 400°C, all of the blocks heat-fractured and the experiment was terminated.

Flakes were knapped at room temperature from each nodule after every heating stage. We used organic and soft-stone hammer percussion. The removal was constrained by the volume of chert blocks, so we produced thin flakes (1 to 5 mm thick), not exceeding 50 mm in length. By this, we obtained 12 flakes of each block of raw material (tab.1) (20 for Bergerac chert from Mouleydier). In total, the reference collection contained 80 flakes.

To detect changes in surface roughness, we used a laser scanning microscope (LSM): Keyence VK-100, using a 20x objective at the Competence Center Archaeometry - Baden-Wuerttemberg (CCA-BW) at Tübingen University's Department of Geosciences (aided by C. Berthold and K.G. Nickel). LSM analysis allows for non-contact acquisition of a 3D model representing the surface of the object. Roughness and volume parameters can be extracted from this model. 3D models were acquired on the flakes' ventral faces. These LSM analyses produced 1300 x 960 µm wide models (stitching together four 650 x 480 µm wide tiles for each sample).

Figure 2 shows two examples of 3D surface models of chert fracture surfaces before (fig. 2.a, c) and after heat treatment (fig. 2.b, d). Models were processed using the Gwyddion software package. First we corrected the surface for inclination. Then, without any other filter, we measured the arithmetical mean roughness (Ra; the average height difference of each point compared to the arithmetical mean of the profile; here in nm) from three profiles that were arbitrarily positioned within the surface model (avoiding sample edges, inclusions or holes in the surface). The profiles were arbitrarily chosen and randomly oriented. Their length was not always the same, ranging from 900 to 1000 µm. Resolution of these profiles is a function of the pixel size of the 3D surface files. These measurements were repeated using three different cut-off filters: 0.07 µm, 0.10 µm, 0.15 µm. In Ra measurements, cut-off filters are used to exclude the waviness of the surface (i.e. the larger-scale height differences). Practically, this means the algorithm draws straight baselines between set distances on the profile, to then measure the vertical distance of each point on the profile from these baselines. A cut-off filter of 0.07 µm for example means the baselines were 0.07 µm long. We choose to test three different values of cut-off filters to see if one was more appropriate. All Ra values obtained from each of the three cut-off filtered profiles are presented in table 1. The data plot in Figure 3 thus consist of 9 measurements for each temperature step: tree Ra values from 2D profile measurement made on each of the tree flakes knapped from chert heated to that temperature.

Results

Ra values are summarized in Table 1. Data are visually presented for each raw material and temperature step in Figure 3 (for data extracted using a cut-off filter 0.15 µm). Regardless of the selected cut-off, the trend in the evolution of roughness as a function of temperature is similar. Results vary depending on raw material. Four of the six chert samples (Bergerac, Grand Pressigny and Senonian Fleurac) show similar trends, from high initial Ra to decreasing Ra after heat treatment at 200-300°C. In three of these four samples, Ra is rising again after heating to 400°C. The other two samples yielded unclear results, although the same trend may be interpreted as also being visible in Senonian Chert from Saint Circ.

Discussion and conclusion

LSM analyses confirm the evolution of fracture surface roughness as a function of heating, although, due to the reduced sample size, these results should be interpreted with caution. At 400°C, the increase in Ra seen in three (perhaps 4 if the trend observable for Saint Circ chert is included) of the samples might be explained by the micro-fractures (**Schmidt et al. 2011; Schmidt, 2017**). Micro-fracturing creates "predetermined fracture points", deviating the propagating conchoidal fractures from their ideal path (**Flenniken and Garrison, 1975**). This can be expected to lower knapping quality (overheating, **Schmidt, 2014**). Not all samples seem to be similarly affected by overheating, reflecting the different chemical transformations reported in different chert types (**Schmidt et al., 2012**) that most likely go hand in hand with differing mechanical transformation. During flakes removal, we observed an improvement in knapping quality of most cherts between 200 and 300°C. Yet, for the Vierzon Turonian chert and the Senonian chert from Fleurac, no knapping quality changes were observable. At 400°C, cherts blocks (except Bergerac chert from Mouleydier) presented signs of overheating, such as like pot-lids, and knapping quality tend to decrease.

Raw material type also seems to influence the overall Ra value and its relative evolution. This is in agreement with macroscopic observations of the surfaces we made during the experiments: depending on raw material, macroscopically visual gloss does not appear at the same temperature and its intensity varies in different samples. For example, for the Turonian chert of Vierzon, no clear evolution of the gloss as a function of temperature is macroscopically observable. This could explain the poor evolution of the roughness measurements for this raw material (fig.3). Ra therefore seems to be a good proxy for visual gloss on heat-treated chert. Furthermore, Ra reduction is gradual in the temperature zone where chert is transformed during heat treatment. Our results are encouraging because they provide a new measurable phenomenon revealing the thermal transformations in chert. Measuring Ra non-destructively is a simple way to quantify the evolution of mechanical changes in rocks upon heating. Also, contrary to visual observations, phenomena that influence the reflectance of light (i.e. the proportion of light reflected back from a surface), other than roughness, are not taken into account by Ra measurements. This is so because reflectance is a function (as given by the Fresnel equations) of physical properties absorption coefficient and refractive index. Both are different in different minerals. Non-quartz mineral inclusions in chert therefore may cause differences in light reflectance, even if the roughness of the surface is the same. Ra measurements using LSA are not affected by this phenomenon. This method could become a new tool for the recognition of heat treatment, when visual evaluation alone is not conclusive (in the absence of pre- and post heating scars on the same surface). However, the data are still not statistically relevant enough to be used for this purpose and should only be considered with caution.

As it stands, these first results pinpoint the potential of Ra measurements for the study of post-heat treatment knapping, while demanding future, more systematic analyses of a wider range of samples and a more resolved set of temperature steps.

References

Bordes, F., 1969. Traitement thermique du silex au Solutréen, Bulletin de la Société préhistorique française 66, 197.

Collins, M.B., Fenwick, J.M., 1974. Heat Treating of Chert: Methods of Interpretation and Their Application. Plains Anthropologist 19, 134–145. https://doi.org/10.1080/2052546.1974.11908696

Flenniken, J.J., Garrison, E.G., 1975. Thermally Altered Novaculite and Stone Tool Manufacturing Techniques. Journal of Field Archaeology 2, 125. https://doi.org/10.2307/529623

Griffiths, D.R., Bergman, C.A., Clayton, C.J., Ohnuma, K., Robins, G.V., 1987. Experimental investigation of the heat treatment of flint, in: Sieveking, G.d.G., Newcomer, M.H. (Eds.), The human uses of flint and chert. Proceedings of the fourth international flint symposium held at Brighton Polytechnic 10-15 April 1983, Cambridge University Press, Cambridge, 43 - 52.

Inizan, M.-L., Roche, H., Tixier, J., 1976. Avantage d'un traitement thermique pour la taille des roches siliceuses. Quaternaria XIX, 1–18.

Masson, A., 1981. Le comportement thermique du silex: application. Staringia 96–98.

Rondeau, M.F., 1995. Thermal damage does not equal heat treatment, Lithic Technology 20, 135 - 136.

Schmidt, P., 2013. Le traitement thermique des matières premières lithiques : Que se passe-t-il lors de la chauffe ?, Archaeopress, BAR International Series 2470, Oxford.

Schmidt, P., 2014. What causes failure (overheating) during lithic heat treatment?, Archaeol Anthropol Sci 6, 107-112.

Schmidt, P., 2017. How reliable is the visual identification of heat treatment on silcrete? A quantitative verification with a new method. Archaeological and Anthropological Sciences. 11, 713–726. https://doi.org/10.1007/s12520-017-0566-6

Schmidt, P., Badou, A., Fröhlich, F., 2011. Detailed FT near-infrared study of the behaviour of water and hydroxyl in sedimentary length-fast chalcedony, SiO2, upon heat treatment, Spectrochimica Acta Part A: Molecular and Biomolecular Spectroscopy 81, 552-559.

Schmidt, P., Buck, G., Berthold, C., Lauer, C., Nickel, K.G., 2019. The mechanical properties of heat-treated rocks: a comparison between chert and silcrete. Archaeol Anthropol Sci 11, 2489–2506. https://doi.org/10.1007/s12520-018-0710-y

Schmidt, P., Paris, C., Bellot-Gurlet, L., 2016. The investment in time needed for heat treatment of flint and chert. Archaeological and Anthropological Sciences 8, 839–848. https://doi.org/10.1007/s12520-015-0259-y

Schmidt, P., Masse, S., Laurent, G., Slodczyk, A., Le Bourhis, E., Perrenoud, C., Livage, J., Fröhlich, F., 2012. Crystallographic and structural transformations of sedimentary chalcedony in flint upon heat treatment. Journal of Archaeological Science 39, 135–144. https://doi.org/10.1016/j.jas.2011.09.012

Tiffagom, M., 1998. Témoignages d'un traitement thermique des feuilles de laurier dans le Solutréen supérieur de la grotte du Parpalló (Gandia, Espagne). Paléo 10, 147–161. https://doi.org/10.3406/pal.1998.1134

Table 1. Ra values obtained from each of the three cut-off filtered profiles (0.07, 0.10 and 0.15 µm).

Chert type	Temperature	Sample	Ra (cut-off = 0.07)			Ra (cut-off = 0.10)			Ra (cut-off = 0.15)		
Bergerac chert (Mouleydier)	Not Heated	1	727.7	704.5	796.9	687.7	678.1	757.1	591.8	636.1	682.2
	Not Heated	2	724.5	700.9	693.5	646.7	653.3	627.1	595	619.9	586.8
	Not Heated	3	741.7	708.6	711.2	695.8	674.2	675.6	611.8	592.4	615.2
	Not Heated	4	71.7	765.5	744	682.1	700	706.3	648.7	601.2	608.6
	Not Heated	5	652	680.9	681.1	596.5	646.5	627.2	518.2	598.2	562.8
	200°C	1	630.6	716.8	634.5	583.5	670.8	583	520.5	587.8	543.5
	200°C	2	583	689.6	613.2	562.3	641	572.3	522.7	542.9	510.1
	200°C	3	710.2	629.2	588.5	626.3	532.9	521.4	523.7	487.6	445.3
	200°C	4	875	721.6	808	824.9	649.1	737.2	679.1	586.1	604.6
	200°C	5	777	700.9	835	736	627.4	763.9	621	563	694.9
	300°C	1	655.1	532.9	563.4	603.4	498.8	534.1	533.5	446.5	474.9
	300°C	2	426.1	474.3	461.8	404.5	445.9	421.7	363.3	385.7	369.1
	300°C	3	545.9	504.4	494.9	499.4	466.4	458.3	432.3	421.4	416.5
	300°C	4	587.9	518.7	599	540.5	493.3	568	500.4	438.6	537.4
	300°C	5	557.9	582.3	600	540.9	554.6	551.7	490.3	501.3	508.1
	400°C	1	445.5	494	574	394.4	439.5	492.4	348.1	365.6	437.5
	400°C	2	688.6	540	576.1	626	485.2	529.2	526.9	417.2	444.5
	400°C	3	678.4	730	737.7	597.4	687.3	667.4	491.6	574.8	565.3
	400°C	4	519.2	496.4	481.7	436.8	455	447.4	364.2	385.1	352.3
	400°C	5	592.5	582.3	568	550.9	534.7	548.3	478.3	467	481.1
Senonian chert (St Circ)	Not Heated	1	680.3	718.5	755.1	627.9	646.6	699.9	573	554.2	626
	Not Heated	2	704.3	727.5	626	636.3	698.6	604.2	603.7	604.5	565.2
	Not Heated	3	688.9	698.3	680.1	640.6	672.6	646.6	565.8	627.4	581.2
	200°C	1	527.8	609.2	579.5	500.6	577	555.8	437.7	505.8	482.4
	200°C	2	564	576.3	489.5	547.9	539.4	460.1	482.8	490.8	423.1
	200°C	3	599.5	613.9	561.1	576.2	580.7	515.9	500.4	532.7	457.2
	300°C	1	627	618.6	615.6	589.4	588.9	574.5	514	546.7	527
	300°C	2	506.8	512.8	528	452.5	487.6	489.6	388.5	452.9	413
	300°C	3	633.9	750	644.8	598	713.5	611.1	531	652.7	561.4
	400°C	1	664	705	688.9	646.1	662.2	658.9	580.1	603.5	613
	400°C	2	659.8	696.9	697	568.1	645	603	504.1	590	497.4
	400°C	3	591.4	660.3	609.2	549.6	604.5	555	471.2	532.4	475.2
Senonian chert (Fleurac)	Not Heated	1	608.4	532.4	538.9	579.8	500.7	516.2	508.9	459.7	478.4
	Not Heated	2	630.2	624.5	763.2	550.1	572.7	684.1	487.9	510.5	561.8
	Not Heated	3	580.4	682.2	620.1	545.1	632.8	575.2	506.6	569.4	501.8
	200°C	1	646.1	628.8	585.5	560.5	578.8	535.7	491.2	518.8	477
	200°C	2	624.6	717.9	734.3	573.2	666	594.1	519.8	570.5	485.9
	200°C	3	754.5	623.2	702.5	668.8	584.7	634.5	563.2	527.3	568
	300°C	1	452.4	529.8	530.4	391.5	456.1	466.6	331.1	386.9	375.3
	300°C	2	541.8	522.6	567.2	500.8	483.9	524.3	416.5	431	451.3
	300°C	3	608.8	588.8	631.8	544.9	539.4	555.4	475.2	483.7	513.7
	400°C	1	674.5	637.5	591.4	617.7	588	546.2	480.1	523.6	476.5
	400°C	2	617	706.3	614	572.4	645.6	569.2	504.2	560	504.4
	400°C	3	666.9	954	651	594.7	835.7	605.2	506.3	622.8	532.4
Bergerac chert	Not Heated	1	734.8	734.5	701.6	685.4	671.6	667.7	637.4	623.9	629.3

(Creysse)	Not Heated	2	640.4	611.5	601.2	614.4	582.2	572.9	559.8	541.4	534.5
	Not Heated	3	671.4	610.5	680.5	636.2	584.9	656.1	586.5	532.6	579.7
	200°C	1	543.2	572.3	558.5	501.1	550.8	527.1	446	517.1	490.6
	200°C	2	768	680.7	655.1	699.5	632.7	600.3	582	559.3	520
	200°C	3	637.3	599	652	609.2	554.5	623.5	540.2	496.6	556
	300°C	1	397	431.1	481.3	363	390.1	436.8	318.8	340.1	367.1
	300°C	2	485.7	444.2	453.8	443.9	425.1	433	396.2	395.6	381.7
	300°C	3	471.7	497.1	518.5	435.8	446	480.2	398	405.8	412.1
	400°C	1	623.7	580.7	689.6	537.3	551.2	631.2	452.2	507.4	550.7
	400°C	2	625.2	634	594.9	595.1	585.8	552	544.1	521.7	523.9
	400°C	3	723	710.4	657.8	681.7	650.8	589	574.8	566.1	513.4
Upper Turonian chert (Le Grand Pressigny)	Not Heated	1	639.6	610.3	608.1	592.2	568.4	563.2	563.2	512.9	519.8
	Not Heated	2	687.3	740.1	716.6	616.5	696.1	665.3	584.3	642.2	619.1
	Not Heated	3	638.9	588	616.3	595.8	554	579	566	503.6	532.7
	200°C	1	516	522	549.4	498.7	499.5	535.1	451.9	460.3	486.6
	200°C	2	577.4	626.9	609.7	547.5	583.1	576.8	503.8	543.5	532.1
	200°C	3	432.7	455.7	429.7	389	413.7	386.9	338.2	366.4	336.9
	300°C	1	591.2	528.3	587.8	553.8	477.3	550	506.4	439	500.3
	300°C	2	463.1	422.2	383.5	423.7	392.4	342.7	364.1	319.7	274.9
	300°C	3	414	397.9	491.6	391.7	364.7	452.2	353.3	325.3	384.9
	400°C	1	474.9	552.6	528.2	446.1	512.9	469.7	401.5	442.8	415.4
	400°C	2	775.1	801.6	867.5	678.3	684.7	758.8	545.7	524.4	621.7
	400°C	3	641	635.7	585.4	588.2	554.8	544	519.9	474.9	487.1
Lower Turonian chert (Vierzon)	Not Heated	1	607.8	606.8	664.3	598.5	593.1	625.5	542.8	532.1	576.8
	Not Heated	2	625.3	695.4	660.4	597.6	673.9	614.9	559.5	618.8	572.1
	Not Heated	3	671.1	651.5	723.3	630.9	620.8	702.1	576.1	557.5	671.6
	200°C	1	576.7	623	589.4	525.1	570.7	566.3	481.4	538.4	491.7
	200°C	2	619.7	665.9	653.5	564.5	623.9	604.3	505.7	583.9	542.7
	200°C	3	623.7	667.1	611.7	598.8	627.6	576	541.3	575.7	523.9
	300°C	1	604.9	640.7	699.3	536.5	578.8	635.4	473.9	476.2	571.7
	300°C	2	782.5	721	716.4	733.4	656.8	659.6	679.7	569.3	585.9
	300°C	3	438.2	508.1	439.7	414.2	457.1	392.3	369.1	408.6	360.9
	400°C	1	918.5	912	833	857.1	837.2	755.5	752.7	718.8	669.8
	400°C	2	736.1	861.5	769.3	658.8	797	671.4	538.7	701.3	562.1
	400°C	3	582.9	543.3	542.2	536	500.5	471.2	499.3	432.6	412.9

Figure 1. Map of sampled chert source location used for our analysis

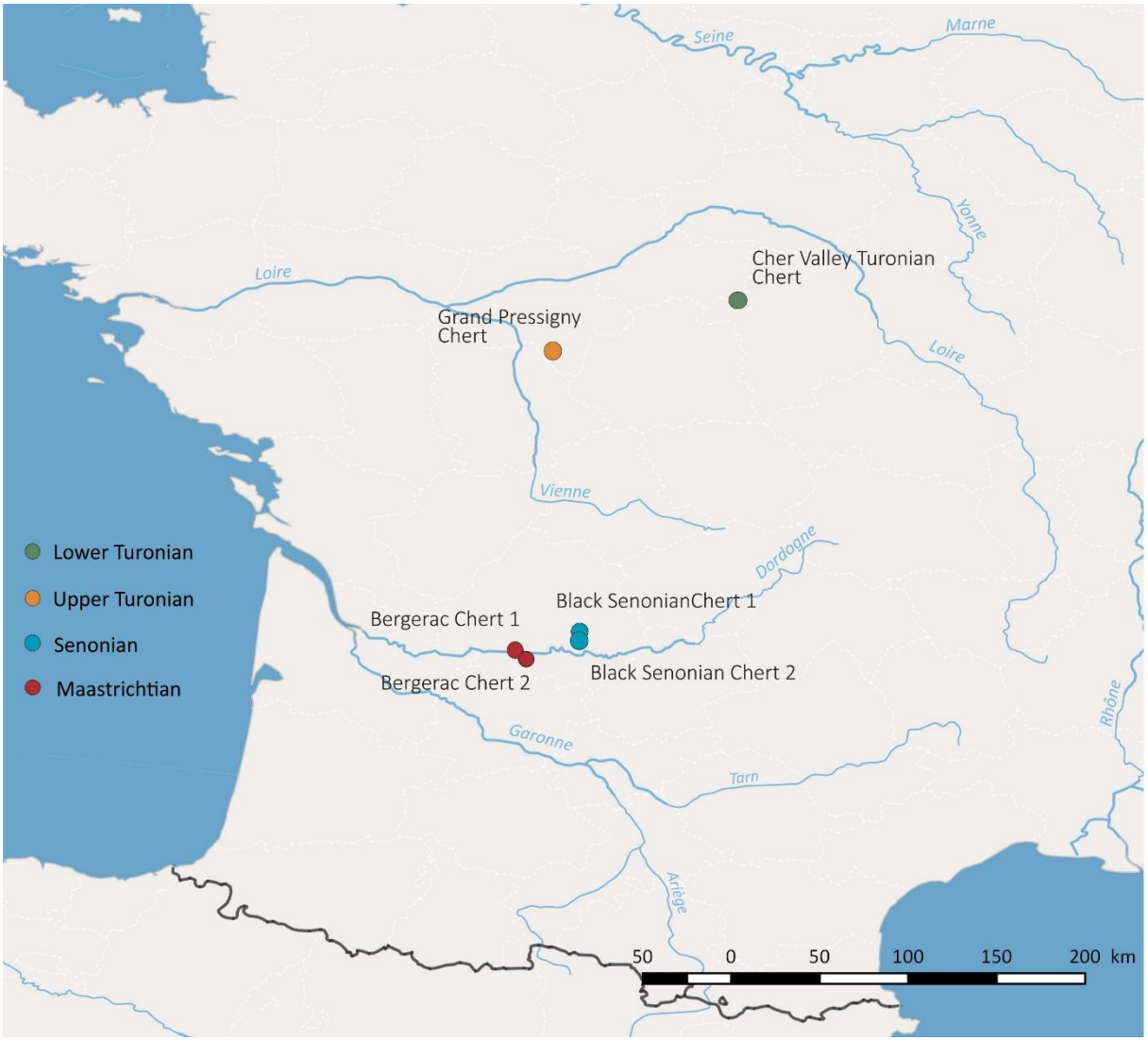

Figure 2. Two surface models as produced by Laser scanning microscopy. (a) 2D representation of a surface data file measures on a relatively rough fracture surface of unheated chert. (b) 2D representational of a surface data file measures on a smoother fracture surface knapped after heating to 300°C. Polynomial background removed from both data files to correct for surface inclination; no other data treatment. (c and d) 3D representations of the same surface data files. Note the different Z scale in both 3D representations that is caused by the different magnitude of the surface roughness before and after heating to 300°C.

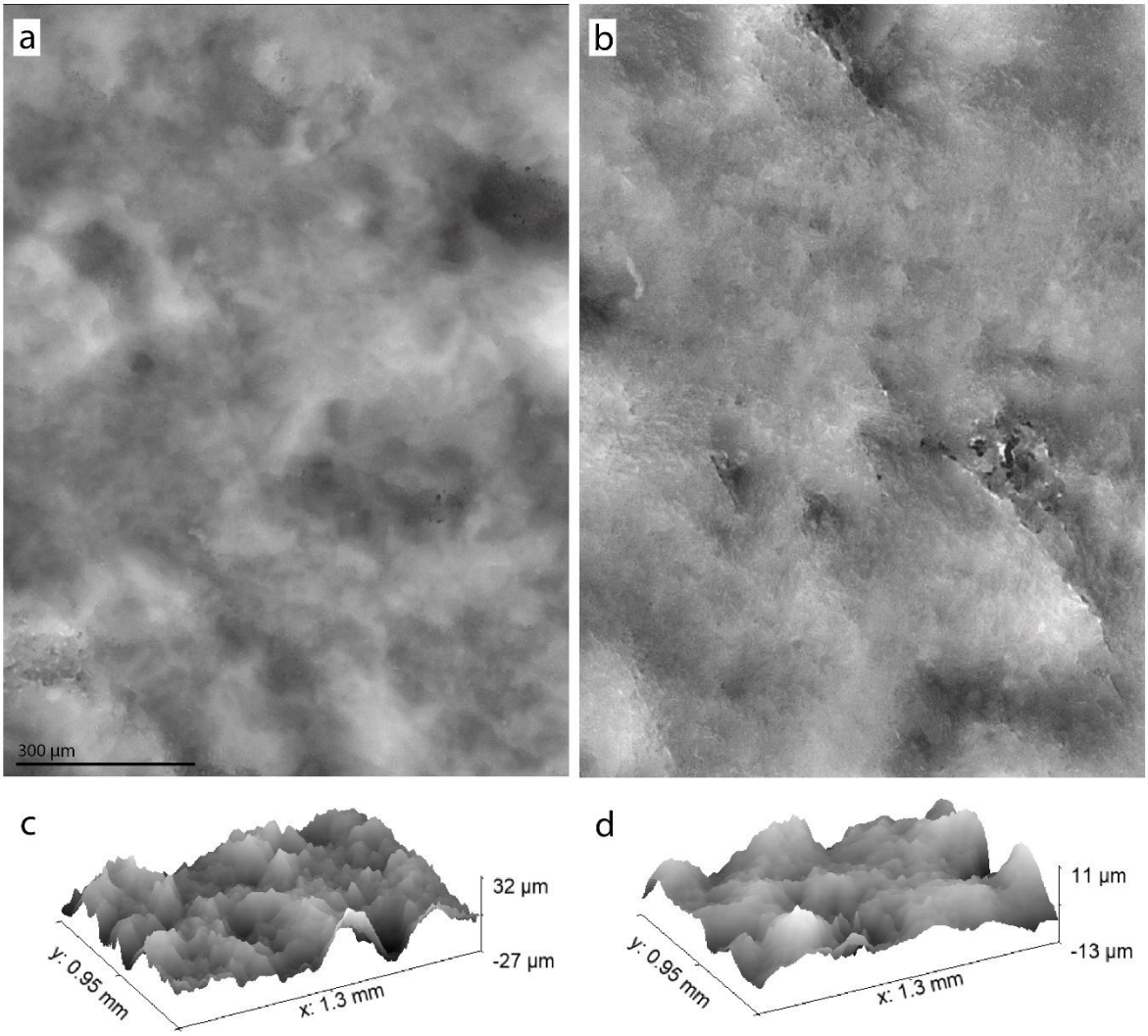

Figure 3. Thermal evolution of surface roughness on different chert types. Gray dots behind the box plot represent the raw data extracted from 2D profiles that were randomly oriented within the lager 3D surface data files shown in Figure 2. No data treatment of surface data files except for applying a cut off filter of 0.15 µm when reading out roughness data from the 2D profiles.